



Laboratoire de Mécanique des Fluides et d'Acoustique
LMFA UMR 5509



ERCOFTAC
European Research Community On
Flow, Turbulence And Combustion

Écully, 7th december 2021

Jet noise modelling by an adjoint statement

Étienne Spieser, Christophe Bailly

ASTROFLU V – ERCOFTAC Workshop

Université de Lyon, École Centrale de Lyon & LMFA



UNIVERSITÉ DE LYON
ÉCOLE
CENTRALE LYON

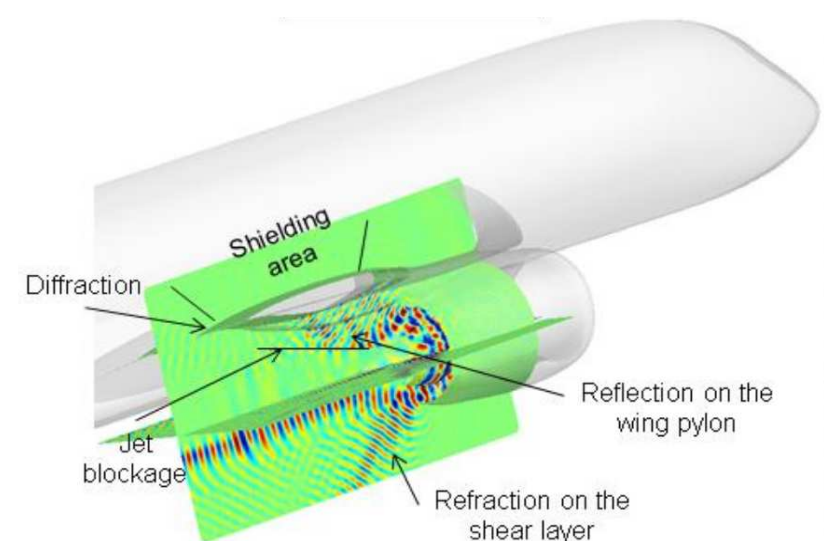
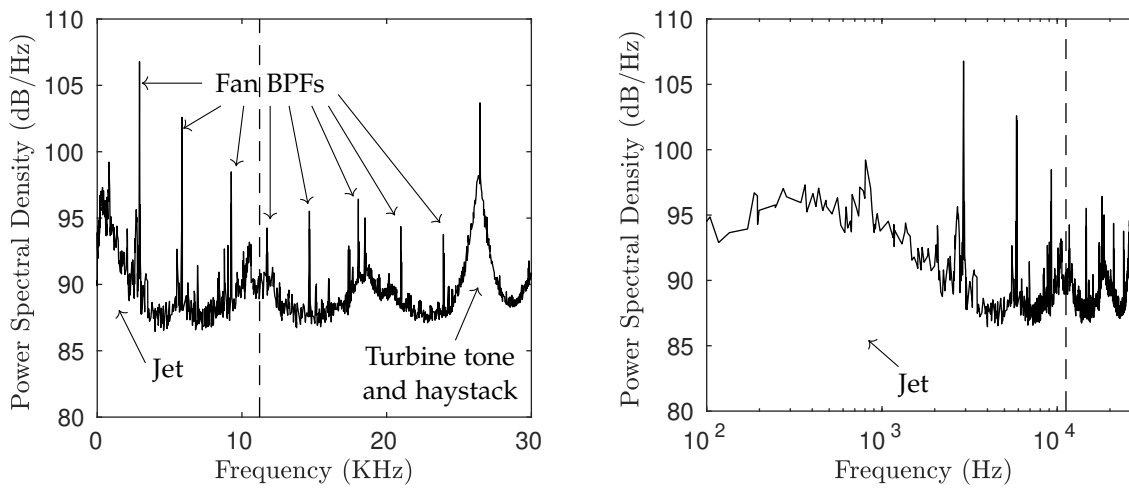
INSA

INSTITUT NATIONAL
DES SCIENCES
APPLIQUÉES
LYON



The acoustic radiation of a turbofan in operation differs greatly from that in ground tests.

Downstream propagation of a fan mode calculated with Actran (Mosson *et al.*, aiaa14).



Jet noise is multi-scale and covers a frequency range of three decades.

Acoustic spectral density for the DGEN 380 at 118° with a BPR of 7.6.

- Statistical modelling in jet noise
- Acoustic prediction of a $M_j = 0.9$ round jet
- Conclusion

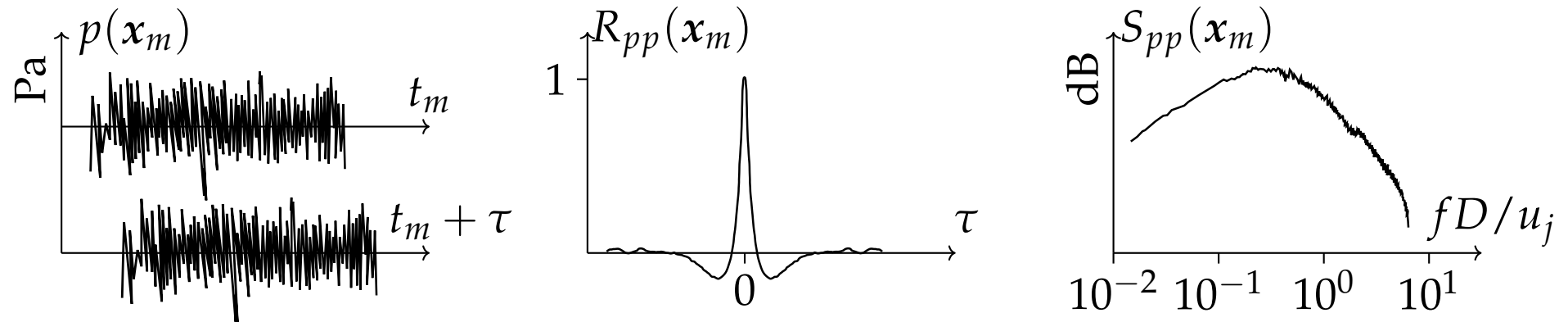
- Statistical description of the acoustic energy

Jet noise is caused by the distortion of turbulent structures.

“Vortex dynamics makes noise” (Powell, jasa64)

Only the average acoustic energy received at the microphone x_m is of relevance,

$$S_{pp}(x_m, \omega) = |p^2(x_m, \omega)|$$



$$R_{pp}(x_m, \tau) = \int_{\mathbb{R}} dt_m p(x_m, t_m)p(x_m, t_m + \tau) \quad \text{and} \quad S_{pp}(x_m, \omega) = \int_{\mathbb{R}} d\tau R_{pp}(x_m, \tau)e^{i\omega\tau}$$

Modelling of the turbulent mixing noise

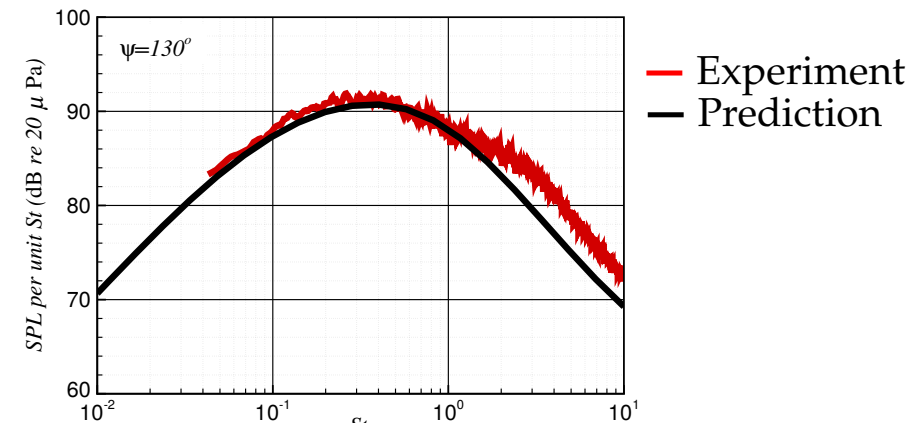
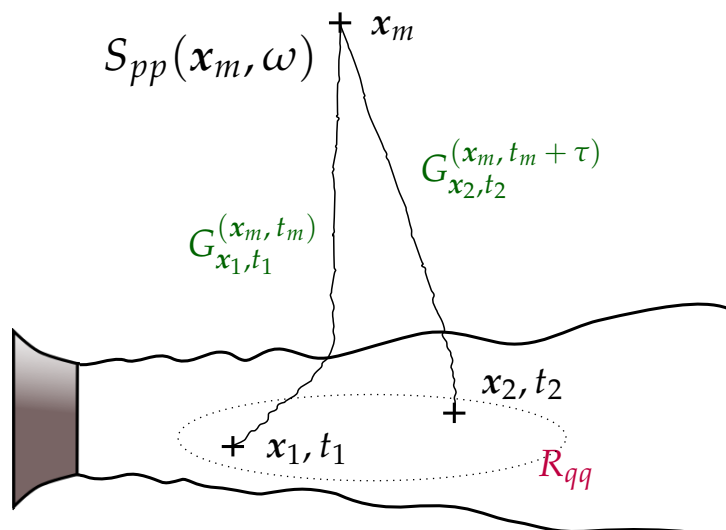
$$S_{pp}(x_m, \omega) = \int_{\mathbb{R}} d\tau \int_{\mathbb{R}} dt_m p(x_m, t_m) p(x_m, t_m + \tau) e^{i\omega\tau}$$

$p(x_m, t_m) = \int_{\mathbb{R}} dt_1 \int_{\Omega} dx_1 G_{x_1}^{(x_m, t_m - t_1)} q(x_1, t_1)$
 $p(x_m, t_m + \tau) = \int_{\mathbb{R}} dt_2 \int_{\Omega} dx_2 G_{x_2}^{(x_m, t_m + \tau - t_2)} q(x_2, t_2)$

$S_{pp}(x_m, \omega) = \int_{\mathbb{R}} d\tau \int_{\mathbb{R}} d\tilde{t}_1 \int_{\mathbb{R}} d\tilde{t}_2 \int_{\Omega} dx_1 \int_{\Omega} dx_2 G_{x_1}^{(x_m, \tilde{t}_1)} G_{x_2}^{(x_m, \tilde{t}_2 + \tau)} R_{qq}(x_1, x_2, \tilde{t}_1 - \tilde{t}_2) e^{i\omega\tau}$

deterministic propagation
statistical sound source

pressure auto-correlation at microphone



S_{pp} from RANS-based Tam and Auriault's mixing noise formula, $M_j = 0.8$ (Miller, 2014)

- Computing the sound propagation with the adjoint

$$S_{pp}(\mathbf{x}_m, \omega) = \int_{\mathbb{R}} d\tau \int_{\mathbb{R}} d\tilde{t}_1 \int_{\mathbb{R}} d\tilde{t}_2 \int_{\Omega} d\mathbf{x}_1 \int_{\Omega} d\mathbf{x}_2 G_{\mathbf{x}_1}^{(\mathbf{x}_m, \tilde{t}_1)} G_{\mathbf{x}_2}^{(\mathbf{x}_m, \tilde{t}_2 + \tau)} R_{qq}(\mathbf{x}_1, \mathbf{x}_2, \tilde{t}_1 - \tilde{t}_2) e^{i\omega\tau}$$

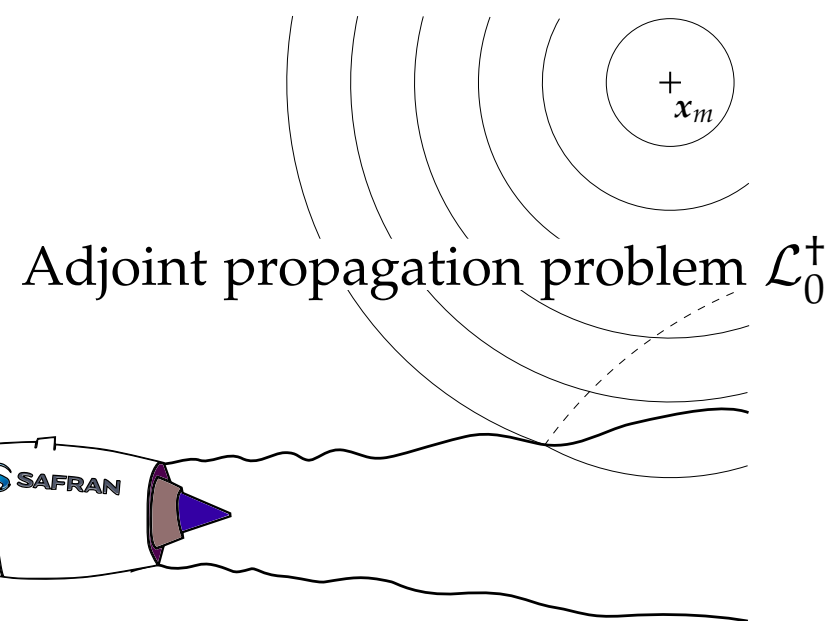
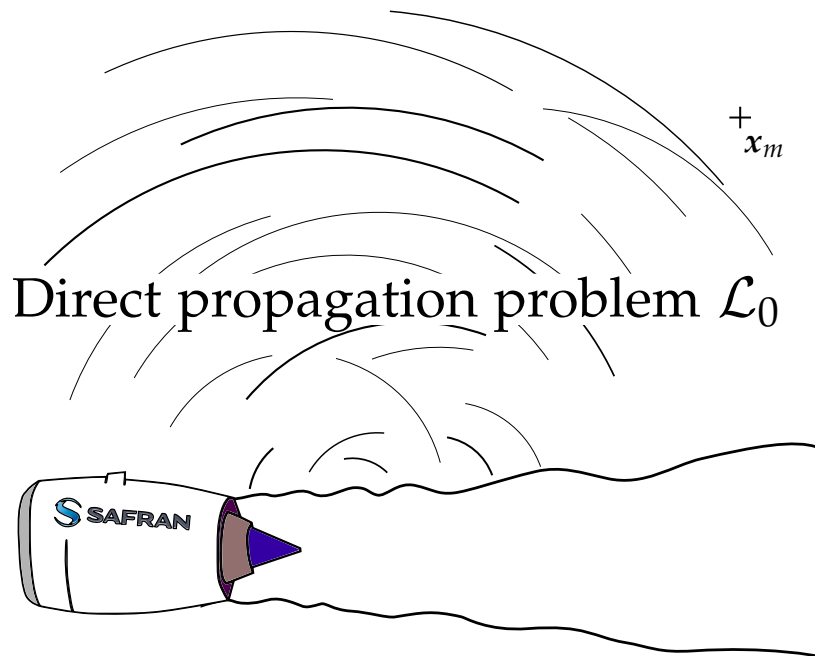
As it is, this formula cannot be used

- Green's functions $G_{\mathbf{x}_1}$, $G_{\mathbf{x}_2}$ must be evaluated for each \mathbf{x}_1 , \mathbf{x}_2 .
- The computational cost of the double volume integral is prohibitive.

Tam and Auriault's model (jfm98, aiaaj99) take advantage on the **adjoint framework** to express the **most general statement of the reciprocity principle**.

$$G_{\mathbf{x}_1, t_1}^{(\mathbf{x}_m, t_m)} = G_{\mathbf{x}_m, t_m}^{\dagger(\mathbf{x}_1, t_1)} \quad G_{\mathbf{x}_2, t_2}^{(\mathbf{x}_m, t_m)} = G_{\mathbf{x}_m, t_m}^{\dagger(\mathbf{x}_2, t_2)}$$

Following the reciprocity principle, the source for the adjoint problem is set in x_m .



To be tailored to complex geometries, numerical Green's functions $G_{x_m}^+$ are required.

- Tam and Auriault's mixing noise model (aiaaj99)

A RANS-informed analytical expression for the sound source auto-correlation R_{qq} ,

$$R_{qq}(\mathbf{r}, \tilde{\tau}) = \frac{A^2}{\tau_s^2} \exp \left(-\frac{|\mathbf{r} \cdot \mathbf{u}_0|}{u_0^2 \tau_s} - \frac{\ln(2)}{l_s^2} (\mathbf{r} - \tilde{\tau} \mathbf{u}_0)^2 \right)$$

the reciprocity principle expressed with the adjoint,

$$\mathbf{G}_{x_s}^{(x_m, \omega)} = \mathbf{G}_{x_m}^{+(x_s, \omega)} {}^*$$

and a Fraunhofer approximation are used to simplify and evaluate the integrals.

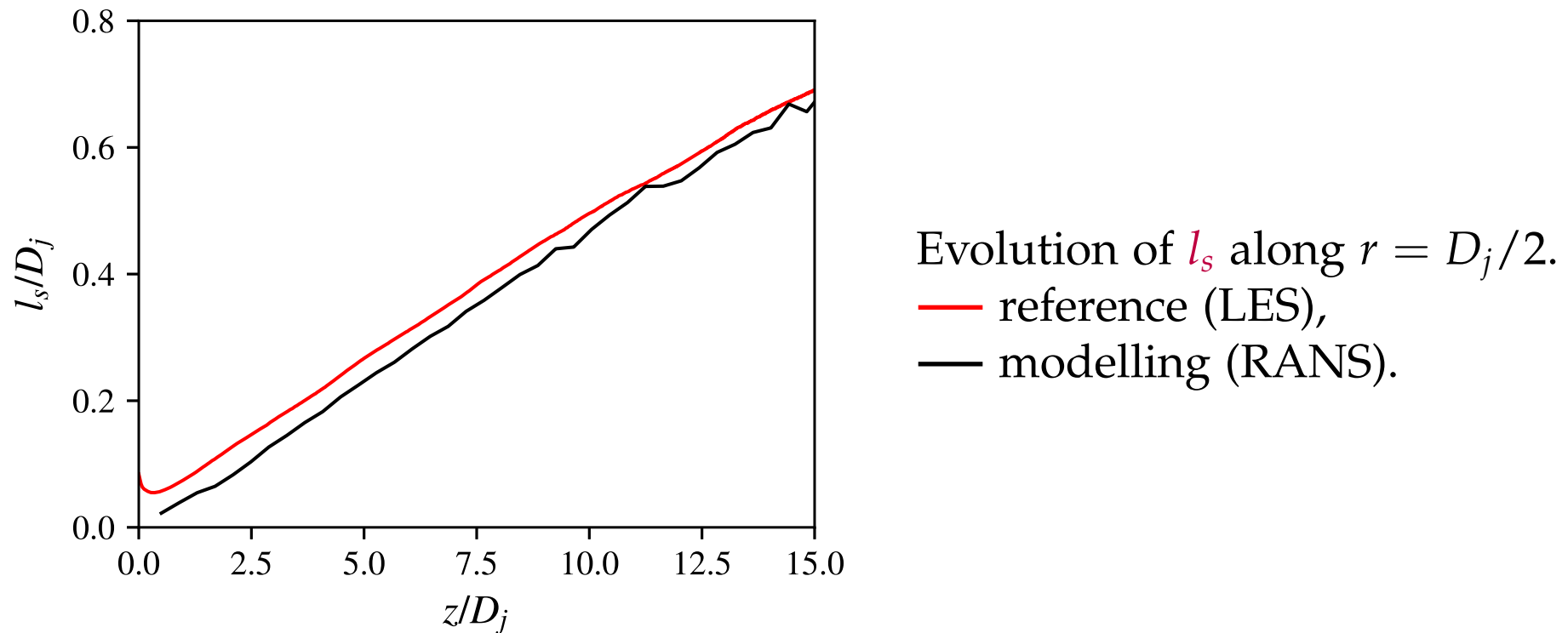
$$S_{pp}(x_m, \omega) = \int_{\Omega} d\mathbf{x}_s \frac{2A^2 l_s^3}{\tau_s} \left(\frac{\pi}{\ln(2)} \right)^{3/2} \left| \mathbf{G}_{x_m}^{+(x_s, \omega)} \right|^2 \frac{\exp \left(\frac{-\omega^2 l_s^2}{4 \ln(2) u_0^2} \left(1 + \frac{u_0^2 |x_{m,\perp}|^2}{a_\infty^2 |x_m|^2} \right) \right)}{1 + \omega^2 \tau_s^2 \left(1 - \frac{\mathbf{u}_0 \cdot \mathbf{x}_m}{a_\infty |\mathbf{x}_m|} \right)^2}$$

- Calibration of the sound source model R_{qq}

The variables A , τ_s and l_s are modelled from the turbulent kinetic energy of the fluid,

$$A \propto \rho_0 k , \quad l_s \propto \sqrt{k} / \left| \frac{\partial u_x}{\partial r} \right| , \quad \tau_s = l_s / u_c \text{ with } u_c = 0.65 u_j$$

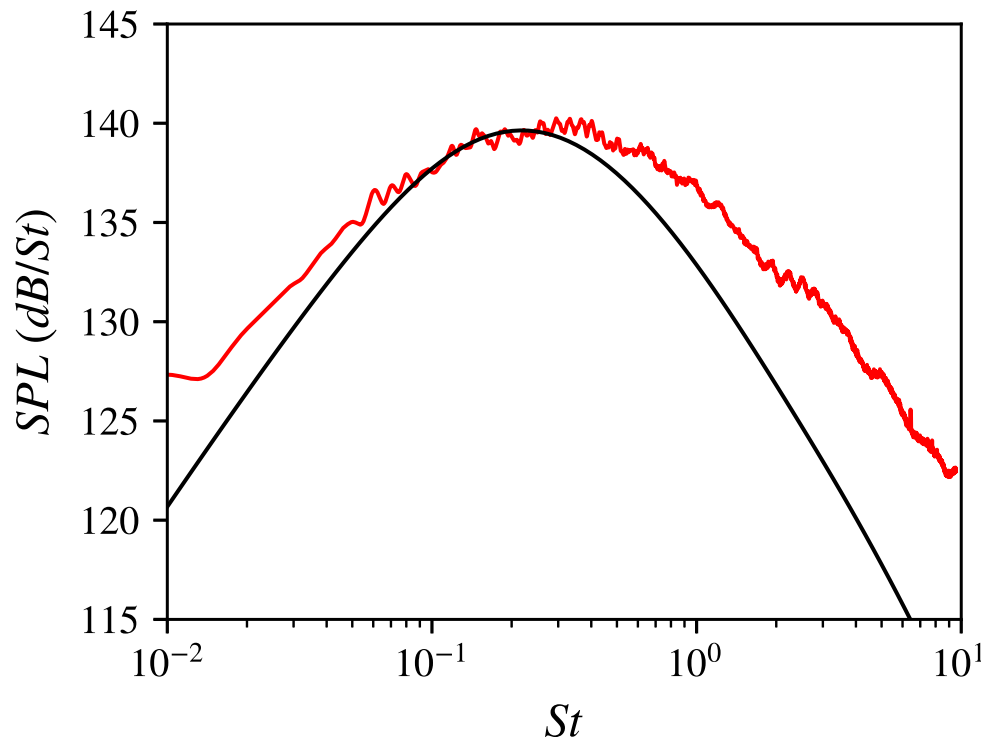
An integral length scale computed from a $M_j = 0.9$ jet LES is used to calibrate l_s .



The source amplitude A is calibrated with the acoustic spectra at 90° , for which,

$$\left| \mathbf{G}_{\mathbf{x}_m}^{+(\mathbf{x}_s, \omega)} \right|^2 = \frac{\omega^2}{16\pi^2 a_0^4 |\mathbf{x}_s - \mathbf{x}_m|^2} \quad (\text{free-field solution})$$

$$S_{pp}(\mathbf{x}_m, \omega) = \int_{\Omega} d\mathbf{x}_s \frac{2A^2 l_s^3}{\tau_s} \left(\frac{\pi}{\ln(2)} \right)^{3/2} \left| \mathbf{G}_{\mathbf{x}_m}^{+(\mathbf{x}_s, \omega)} \right|^2 \frac{\exp \left(\frac{-\omega^2 l_s^2}{4 \ln(2) u_0^2} \left(1 + \frac{u_0^2 |\mathbf{x}_{m,\perp}|^2}{a_\infty^2 |\mathbf{x}_m|^2} \right) \right)}{1 + \omega^2 \tau_s^2 \left(1 - \frac{\mathbf{u}_0 \cdot \mathbf{x}_m}{a_\infty |\mathbf{x}_m|} \right)^2}$$



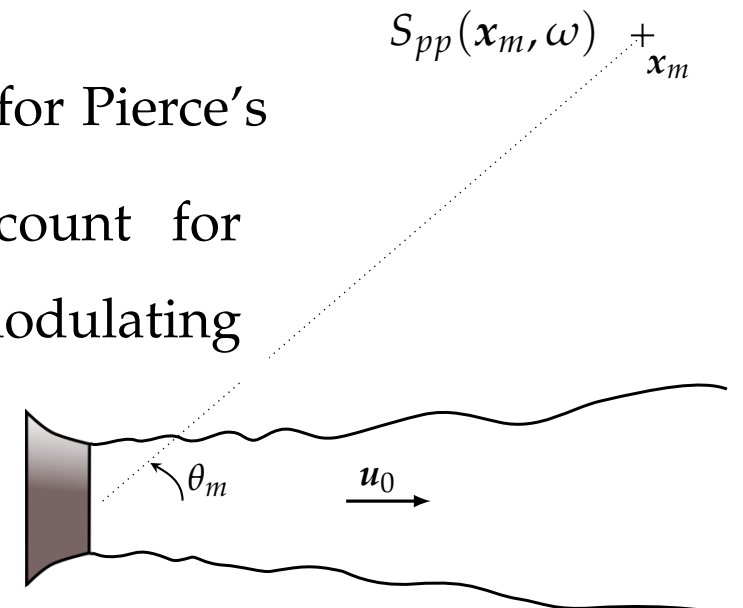
- ECL measurements (Bogey *et al.*, *ija07*),
- prediction, free-field GF.

- Statistical modelling in jet noise
- Acoustic prediction of a $M_j = 0.9$ round jet
- Conclusion

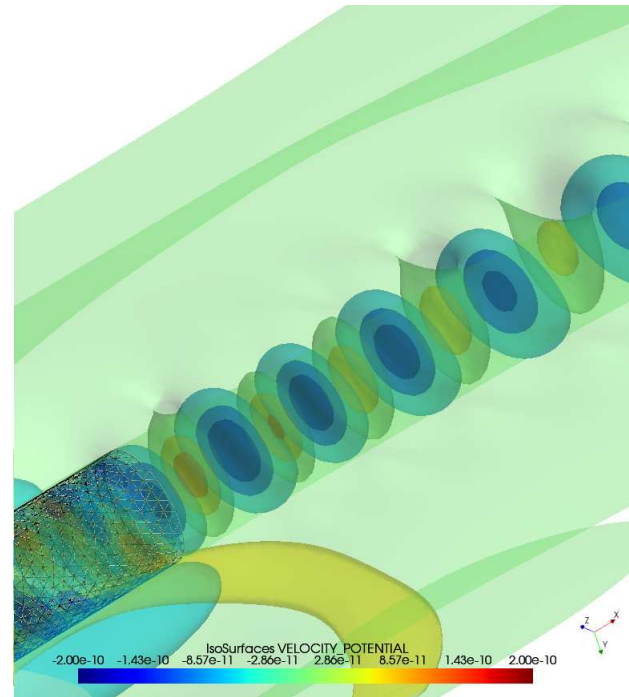
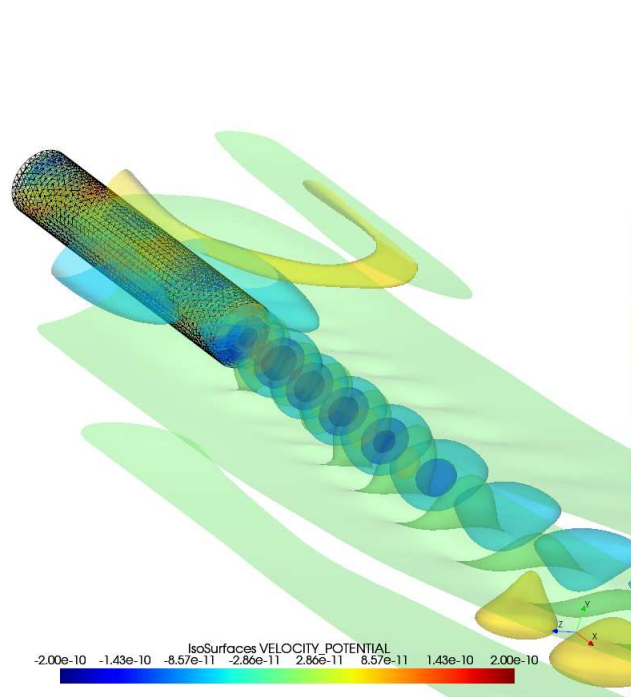
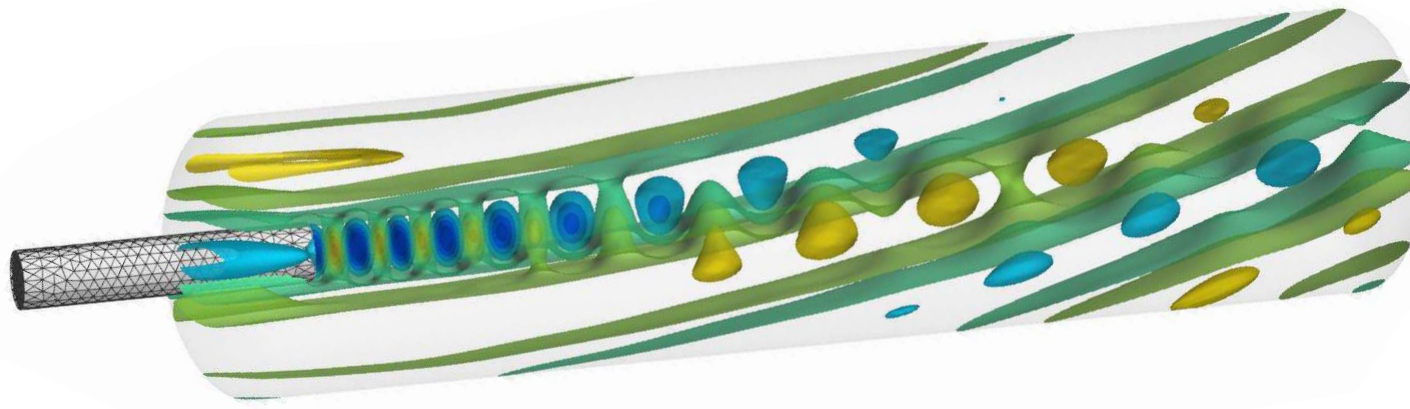
- Implementation for a $M_j = 0.9$ round jet

$$S_{pp}(\mathbf{x}_m, \omega) = \int_{\Omega} d\mathbf{x}_s \frac{2A^2 l_s^3}{\tau_s} \left(\frac{\pi}{\ln(2)} \right)^{3/2} \left| \boxed{\mathbf{G}_{\mathbf{x}_m}^{+(x_s, \omega)}} \right|^2 \frac{\exp \left(\frac{-\omega^2 l_s^2}{4 \ln(2) u_0^2} \left(1 + \frac{u_0^2 |\mathbf{x}_{m,\perp}|^2}{a_\infty^2 |\mathbf{x}_m|^2} \right) \right)}{1 + \omega^2 \tau_s^2 \left(1 - \frac{\mathbf{u}_0 \cdot \mathbf{x}_m}{a_\infty |\mathbf{x}_m|} \right)^2}$$

Adjoint Green's functions $\boxed{\mathbf{G}_{\mathbf{x}_m}^{+(x_s, \omega)}}$ are computed for Pierce's equation considering the *flow reversal theorem* and account for the acoustic propagation toward the observer by modulating the integrand of Tam & Auriault's formula .



- Visualisation for $St = 0.35$ and $\theta_m = 90^\circ$



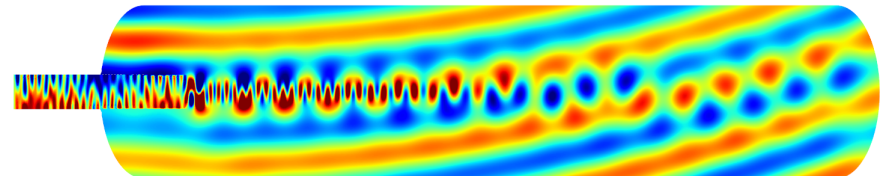
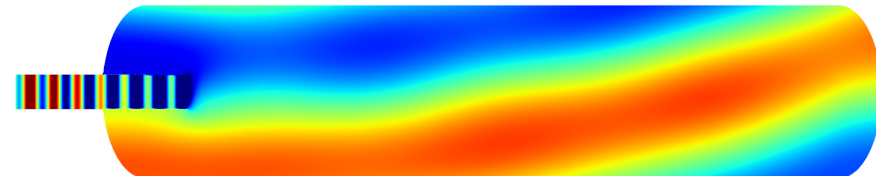
- Adjoint Green's functions

FRT is used and the adjoint source is set at $52D_j$ perpendicular to the jet axis.

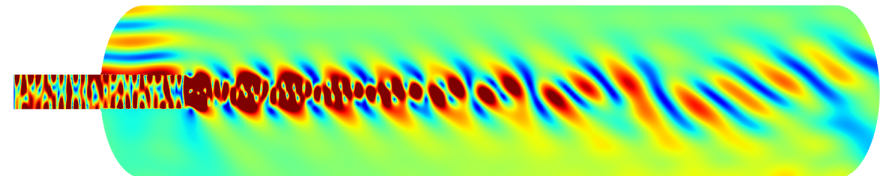
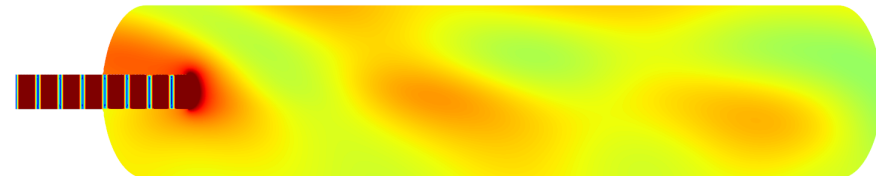
$St = 0.15$

$St = 0.6$

Real part

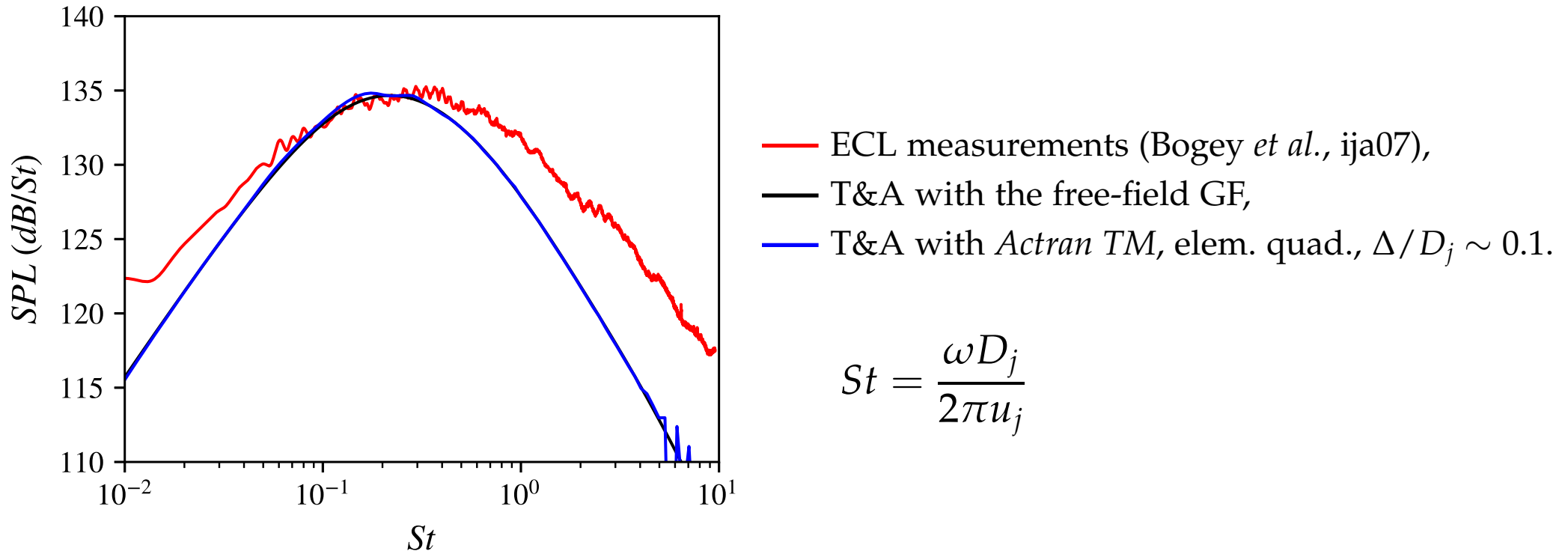


Abs. part



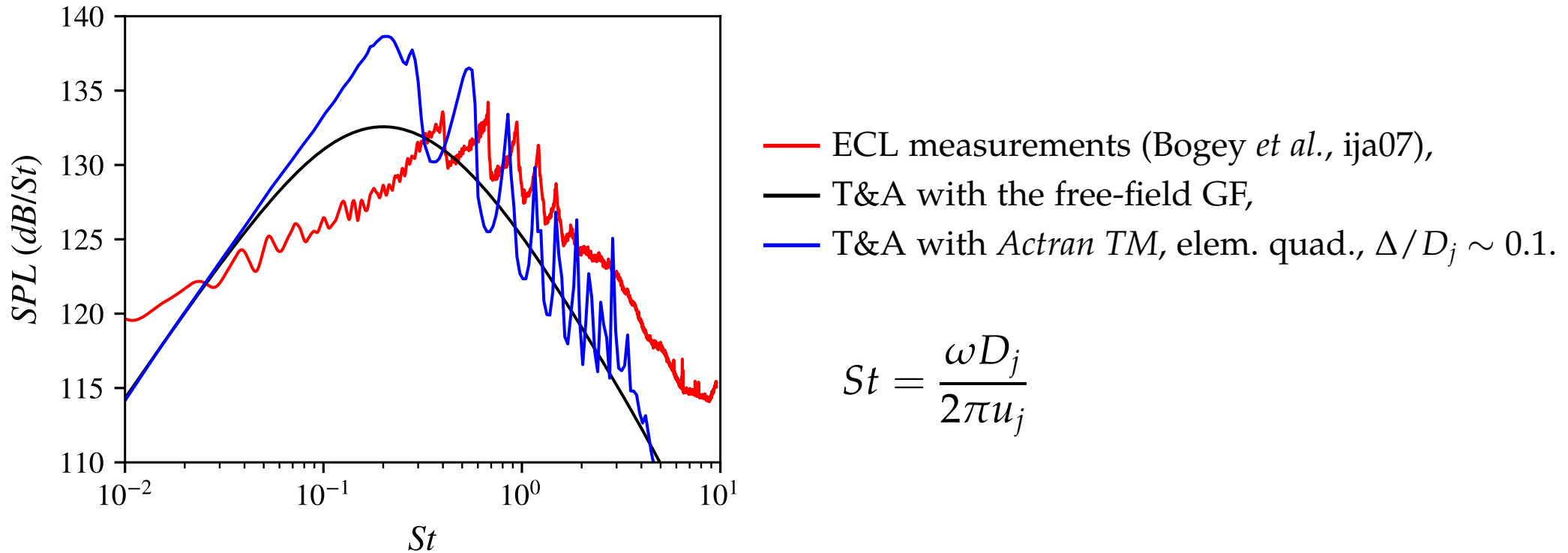
Modal structures appear in the potential cone of the jet and modulate the integrand of Tam and Auriault's formula.

- Noise spectra at 90° for a $M_j = 0.9$ round jet



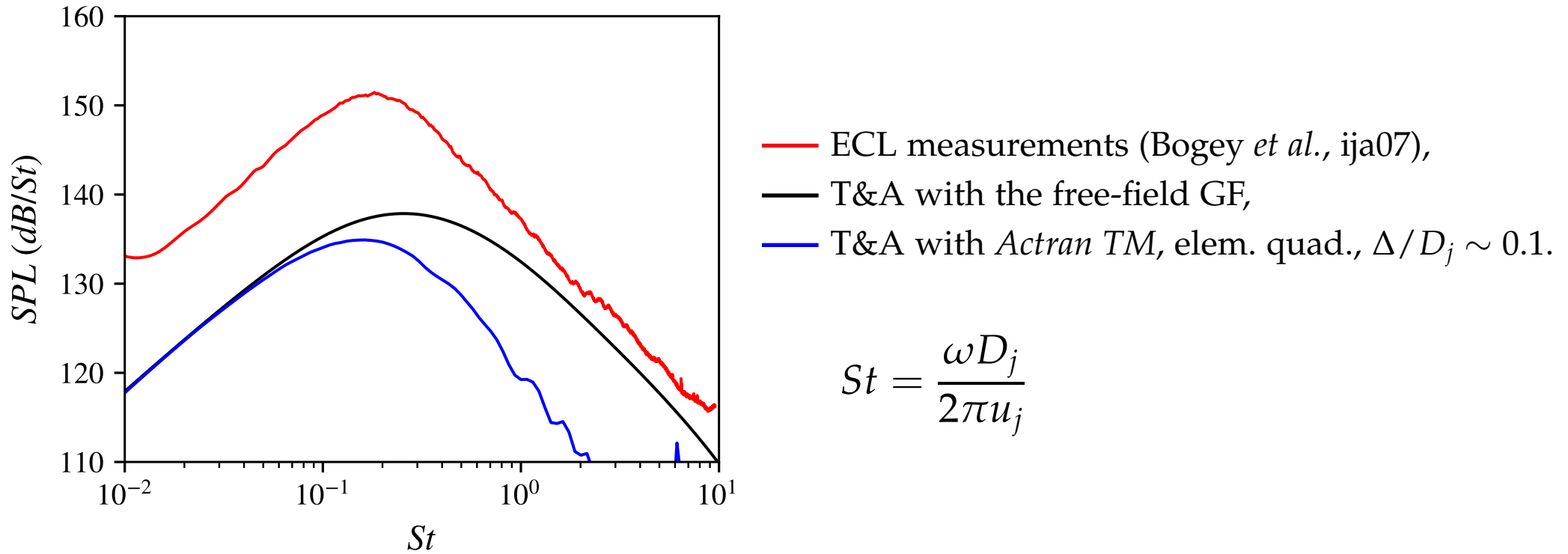
Excellent agreement is obtained between the analytical and numerical prediction.

- Noise spectra at 150° for a $M_j = 0.9$ round jet



Complex phenomena can be described with tailored Green's functions.

- Noise spectra at 30° for a $M_j = 0.9$ round jet



A model to describe *shear-noise* remains to be implemented in the prediction model.

- Statistical modelling in jet noise
- Acoustic prediction of a $M_j = 0.9$ round jet
- Conclusion

- Tam and Auriault's model is recast for potential acoustics. From the self-adjointness the implementation of the adjoint calculation is simplified and guarantee on the stability of the linear propagation problem is given.
- The source model is calibrated using an integral length scale from a LES. Reasonable results are obtained, underlining the physical correctness of the model.
- *Actran TM* is used to calculate the adjoint solution to Pierce's equation, encouraging results are obtained (CPU costs, upper St limit, representativeness).

- *Actran TM* enables the computation of tailored adjoint Green's functions, making it possible to study installation effects.
- This method provides accurate and robust solution to describe the acoustic propagation. Efforts to improve the source model can be undertaken.

└ Thank you! ┐

BACK-UP

- Le choix d'un opérateur auto-adjoint

Être auto-adjoint garantit que **l'énergie se conserve** (Möhring, swing99).

L'adjoint de tels opérateurs peut être calculé par **retournement d'écoulement** (jfm20).

Opérateur auto-adjoint sélectionné : **équation d'onde de Pierce** (jasa90).

$$\frac{D^2\phi}{Dt^2} - \nabla \cdot (a_0^2 \nabla \phi) = \frac{D S_m}{Dt} \quad \text{avec} \quad \begin{cases} \nabla \phi = \rho_0 \mathbf{u} \\ p = -D\phi/Dt \end{cases}$$

et où $\Delta S_m = \nabla \cdot \nabla \cdot (\rho_0 \mathbf{u}' \otimes \mathbf{u}')$ et D/Dt est la dérivée convective.

● Résolution avec *Actran TM*

Actran TM est un code FEM résolvant l'équation de Möhring's normalisée,

$$\frac{D}{Dt} \left(\frac{\rho_0}{\rho_{T,0}^2 a_0^2} \frac{D b}{Dt} \right) - \nabla \cdot \left(\frac{\rho_0}{\rho_{T,0}^2} \nabla b \right) = 0$$

où $\frac{\partial p}{\partial t} = \frac{\rho_0}{\rho_{T,0}} \frac{D b}{Dt}$ et $\rho_{T,0} = \rho_0 \left(1 + \frac{\gamma - 1}{2} M_0^2 \right)^{1/(\gamma-1)}$ est la densité totale.

La transformation $\rho_0 \rightarrow \rho_{0,c}$ et $p_0 \rightarrow p_{0,c}$ permet de retrouver l'équation de Pierce.

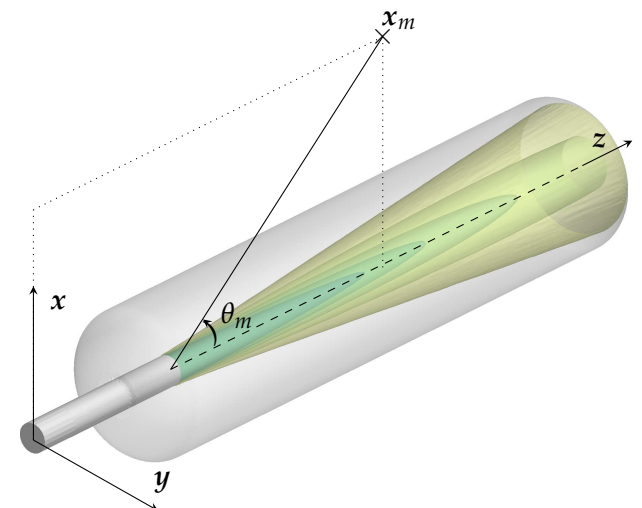
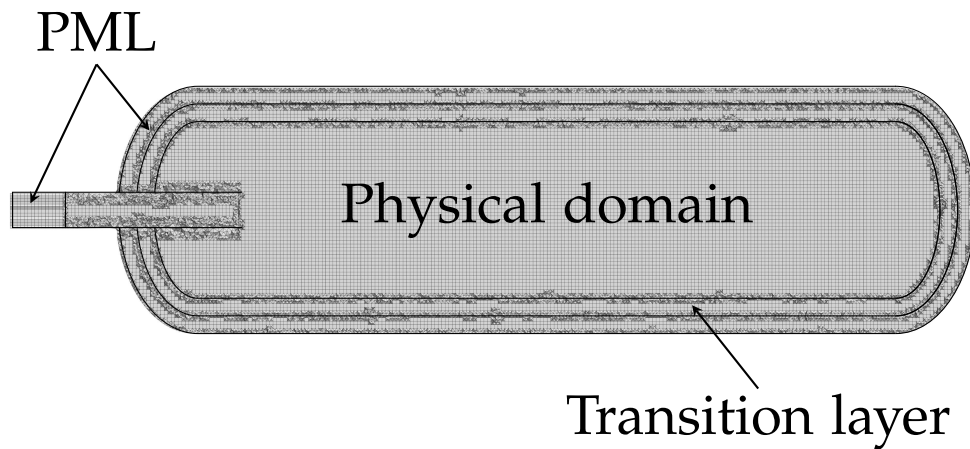
$$\frac{p_{0,c}}{p_0} = \frac{\rho_{0,c}}{\rho_0} = \left[1 + \frac{\gamma - 1}{2} \frac{\mathbf{u}_0^2}{a_0^2} \right]^{-2/(\gamma-1)}$$

L'amplitude doit être corrigée en tenant compte de la vitesse du son $a_{0,s}$ et de l'écoulement $\mathbf{u}_{0,s}$ au voisinage de la source,

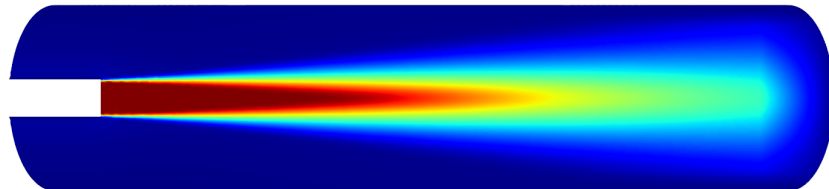
$$\phi = \frac{i\omega}{4\pi a_{0,s}^2} \left(1 + \frac{\gamma - 1}{2} \frac{\mathbf{u}_{0,s}^2}{a_{0,s}^2} \right)^{-1/(\gamma-1)} b^*$$

● Stratégie numérique

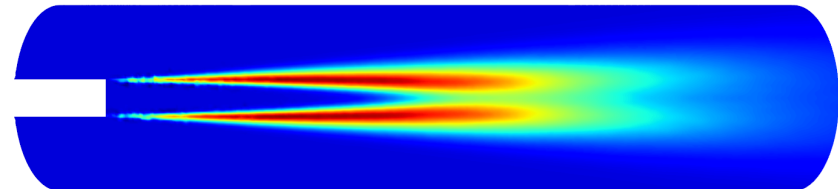
Une procédure pour calculer la solution associée à **une source placée en dehors du domaine discrétré** est développée avec le soutien de C. Legendre (FFT).



Le champ correspondant à un jet à $M_j = 0.9$ est interpolé sur la grille CAA,



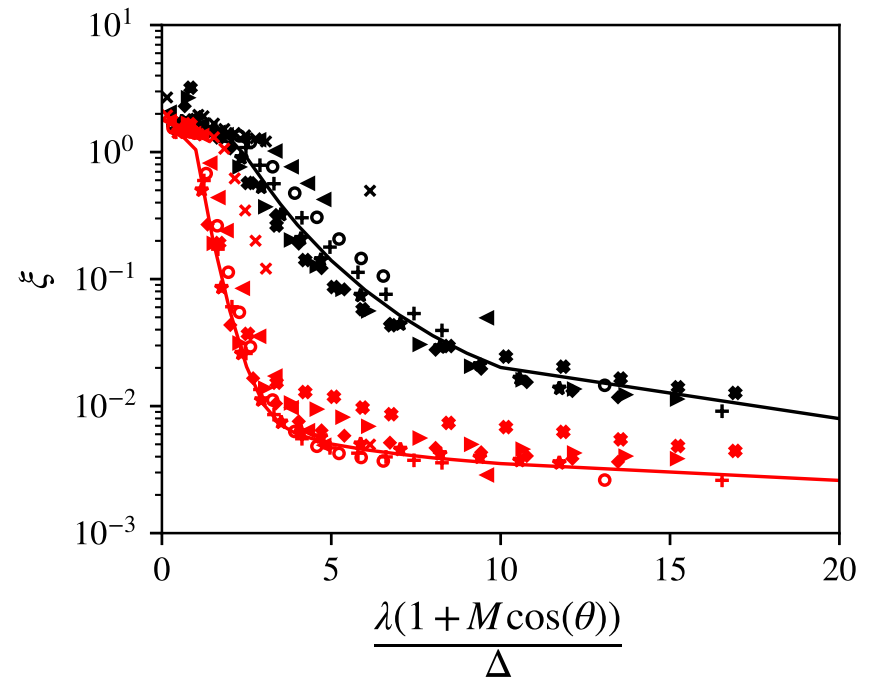
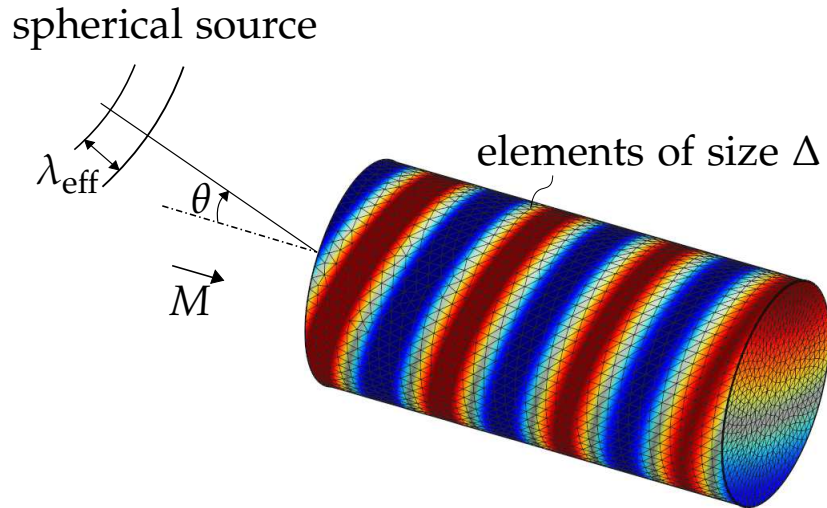
nombre de Mach



énergie cinétique turbulente (TKE)

● Vérification des critères de maillage

La mesure ξ quantifie l'erreur calculée par rapport à la solution analytique pour différentes tailles de mailles Δ .



avec $\lambda_{\text{eff}} = \lambda(1 + M \cos(\theta))$, pour des éléments — d'ordre 1, et, — d'ordre 2.
Différents nombres de Mach avec $\theta = 30^\circ$ sont étudiés,

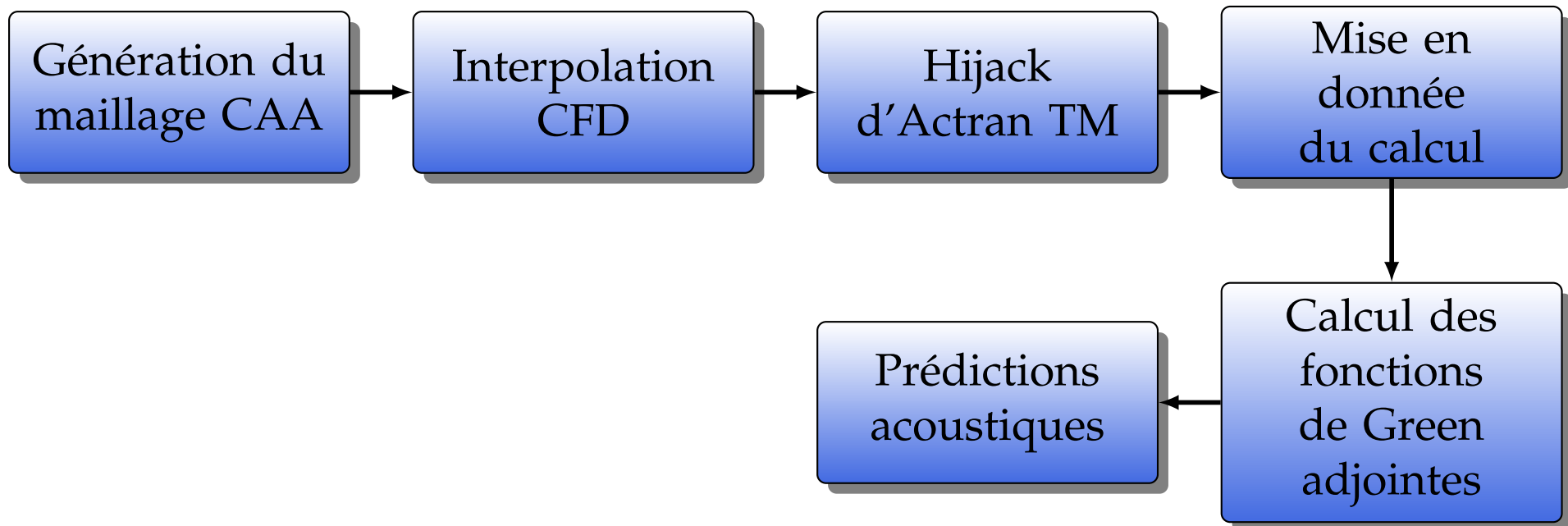
$\times M = -0.8 \blacktriangleleft M = -0.6 \bigcirc M = -0.4 \blacklozenge M = -0.2$ — $M = 0.0 \star M = 0.2 \blacklozenge M = 0.4 \blacktriangleright M = 0.6 \blacktimes M = 0.8$.

- Coûts de calcul

L'algorithme MUMPS en simple précision a été utilisé sur une machine Xenon-Intel E5-2699 @ 2.20 GHz avec 14 threads & 3 processeurs.

element size Δ	DOF	RAM	time for 100 freqs.
$0.5D_j$	0.2×10^6	1.8 GB	1.6 CPU.h
$0.2D_j$	1.7×10^6	13 GB	62 CPU.h
$0.1D_j$	7.7×10^6	75 GB	655 CPU.h
$0.075D_j$	16.2×10^6	178 GB	5500 CPU.h

● Résumé de la mise en oeuvre



L'utilisation d'actranpy permet de rendre cette mise en oeuvre scriptée.

```
Actran_2021.1/bin/actran -u VI -x TA_model.py -n --threads 8
```